Longitudinal Aerodynamic Modeling of the Adaptive Compliant Trailing Edge Flaps on a GIII Airplane and Comparisons to Flight Data

Mark S. Smith[1] and Trong T. Bui[2]
NASA Armstrong Flight Research Center, Edwards, California 93523

Christian A. Garcia[3]
Jacobs Technology, Inc., Edwards, California 93523

and

Stephen B. Cumming[4]
NASA Armstrong Flight Research Center, Edwards, California 93523

A pair of compliant trailing edge flaps was flown on a modified GIII airplane. Prior to flight test, multiple analysis tools of various levels of complexity were used to predict the aerodynamic effects of the flaps. Vortex lattice, full potential flow, and full Navier-Stokes aerodynamic analysis software programs were used for prediction, in addition to another program that used empirical data. After the flight-test series, lift and pitching moment coefficient increments due to the flaps were estimated from flight data and compared to the results of the predictive tools. The predicted lift increments matched flight data well for all predictive tools for small flap deflections. All tools overpredicted lift increments for large flap deflections. The potential flow and Navier-Stokes programs predicted pitching moment coefficient increments better than the other tools.

Nomenclature

ACTE	=	Adaptive Compliant Trailing Edge
AVL	=	Athena Vortex Lattice
CFD	=	Computational Fluid Dynamics
EGI	=	Embedded GPS/INS
GIII	=	Gulfstream III airplane
C_L	=	nondimensional lift coefficient
C_{L_0}	=	zero angle of attack lift coefficient
C_{L_α}	=	lift coefficient derivative with respect to angle of attack
C_{L_B}	=	lift coefficient bias
$C_{L_{de}}$	=	lift coefficient derivative with respect to elevator deflection
C_{L_q}	=	lift coefficient derivative with respect to nondimensional pitch rate

[1] Aerospace Engineer, Aerodynamics and Propulsion Branch, P.O. Box 273 Edwards, CA/MS 2228, Senior Member.
[2] Aerospace Engineer, Aerodynamics and Propulsion Branch, P.O. Box 273 Edwards, CA/MS 2228, Senior Member.
[3] Aerospace Engineer, Aerodynamics and Propulsion Branch, P.O. Box 273 Edwards, CA/MS 2228, Member.
[4] Supervisory Aerospace Engineer, Aerodynamics and Propulsion Branch, P.O. Box 273 Edwards, CA/MS 2228, Senior Member.

C_m = nondimensional pitching moment coefficient
C_{m_B} = pitching moment coefficient bias
$\bar{c}$ = reference chord
de = elevator deflection
q = pitch rate
U = uncertainty
V_∞ = true airspeed
$y+$ = normal distance to the wall in boundary-layer wall units
α = angle of attack
ΔC_L = lift coefficient increment due to flap deflection
ΔC_m = pitching moment coefficient increment due to flap deflection
σ = standard deviation
^ = estimate

I. Introduction

THE Adaptive Compliant Trailing Edge (ACTE) flap is a technology that is being studied in support of the National Aeronautics and Space Administration (NASA) Environmentally Responsible Airplane project, in conjunction with the U.S. Air Force Research Laboratory (Wright-Patterson Air Force Base, Ohio). The flap consists of a main center section that deflects through bending, instead of rotating about a hinge or translating along a track. The leading edge of the center section connects to the wing seamlessly, and the inboard and outboard edges connect to the wing using flexible sections, eliminating gaps that produce acoustic noise and reduce aerodynamic efficiency. The compliant flaps also have the potential to be lighter than and have less mechanical complexity than traditional flaps. To demonstrate the compliant flap technology, ACTE flaps were incorporated on a testbed Gulfstream III (GIII) airplane (Gulfstream Aerospace Corporation, Savannah, Georgia).[1] A series of flights was flown at NASA Armstrong Flight Research Center (Edwards, California) with the modified GIII airplane, to obtain aerodynamic and structural data. The flaps were adjustable on the ground only. A photo of the test airplane with the ACTE flaps installed is shown in Fig. 1.

Prior to the research flights, effects of the flaps on the GIII aerodynamic characteristics were predicted, and an aerodynamic model was created from the predictions. The model was used for safety of flight studies and incorporated into a six-degree-of-freedom GIII simulation to assist with pilot training. The model was also used to guide the creation of takeoff and landing charts for the pilots, as well as tables used in the control room during flights for monitoring trim angle of attack and test point speed requirements. The complexity of the model evolved over time in an attempt to make the best use of schedule and resources. The initial model was created with lower-complexity empirical and vortex lattice tools, while higher-complexity analyses were being performed with full potential and Navier-Stokes computational fluid dynamics (CFD) programs. The final model completed before flights began was based solely on the Navier-Stokes CFD results.

This report presents comparisons of the aerodynamic effects of the ACTE flaps estimated from flight data to the effects predicted by the analysis tools. Specifically, lift and pitching moment coefficient increments due to the flaps throughout their range of deflection are presented. A brief description of each analysis tool is given. The method for estimating coefficient increments from the flight results is described. Comments are given regarding the ability of each analysis tool to predict the effects of the flaps, with regard to Mach number and flap deflection magnitude.

II. Airplane Description

This section describes the baseline test aircraft and the ACTE flaps. Flight research instrumentation is discussed.

A. Test Airplane

The test airplane was a Gulfstream Aerospace Corporation GIII twin-engine airplane that has been modified to serve as a research testbed.[2] The baseline GIII airplane uses Fowler flaps as high-lift devices. For this project, the Fowler flaps were removed and replaced with the ACTE flaps. This modification necessitated the removal of the GIII flight spoilers. A diagram of the GIII airplane with ACTE flaps is shown in Fig. 2. The diagram includes some of the

major dimensions of the airplane and shows the location of the aerodynamic moment reference point. The reference point is notably higher than the center of gravity, but its proximity to the thrust axis lessens the effects of thrust on the pitching moment calculated at the reference point. The GIII airplane has a reference wing area of 934.6 ft^2 and reference span of 75 ft. The reference chord, $\bar{c}$, is 13.78 ft.

Extensive flight research instrumentation was added to the plane. Much of the research instrumentation was for structural measurements on the wings (e.g., strain gauges, accelerometers, and fiber optic strain sensing). The wings were equipped with sensors for static pressure measurements and were tufted for flow visualization. Video cameras were mounted externally on the fuselage to provide views of the wings and tufts. An embedded Global Positioning System (GPS)/Inertial Navigation System (INS) (EGI) was installed and served as the primary source of angular rate, linear acceleration, and Euler angle measurements. Another research-quality inertial measurement unit was used as a secondary source for angular rates and linear accelerations. Four flow angle vanes were mounted on the top part of the nose of the airplane, from which freestream angle of attack and sideslip angle could be calculated. Control surface position measurements were obtained from potentiometers installed on all airplane control surfaces. Although several engine-related parameters were recorded, there were no thrust measurements. Fuel weights were radioed by the aircrew to the control room at the start and end of each flight card. These weights were tabulated and interpolated with time during data processing to provide fuel weight estimates that were used to determine gross weight, center of gravity, and moments of inertia.

The deflection of the GIII horizontal stabilizer is ordinarily scheduled based on the Fowler flap setting. For the ACTE flights, the stabilizer was kept at a deflection of -1 deg, which is the nominal setting for the baseline airplane with zero Fowler flap deflection. All of the pre-flight analyses were done with the stabilizer at -1 deg. Stabilizer deflection is defined as being positive when the trailing edge goes down.

B. ACTE Flaps

An illustration of an ACTE flap is shown in Fig. 3. Each flap consists of two flexible end sections and a center section that is somewhat rigid in the spanwise direction. The leading edge of the center section connects seamlessly to the wing. The center section is deflected through bending, instead of rotating about a hinge or translating on a track. The flexible end sections are referred to as *transition* sections, as they form the transition between the center part of the flap and the traditional wing structure. The overall span of each flap is 18 ft. The flaps are roughly 20 percent of the wing chord.

The ACTE flaps were positioned to the desired deflection before flight and were locked in that position for the entire flight duration. The flap deflection amount is defined as the angle between a line from a reference point to the trailing edge of the undeflected flap and a line from that same reference point to the trailing edge of the deflected flap. The deflection definition is illustrated in Fig. 4. Deflections were set based on mapping the settings of internal structural components to desired surface shapes. After being positioned and locked, the flaps were scanned using a laser scanner to verify they met required surface accuracy requirements. The accuracy requirements were based on smoothness, left-right flap symmetry, and overall matches to computer aided design models of the expected flap shape. The ACTE flaps were not instrumented for deflection measurements, so there is no direct way to determine how the deflections may have changed during flight due to aerodynamic loads. Laser scans of the flaps were performed after flights to determine if the surface deflections had changed from the pre-flight scans. The post-flight scans indicated that the deflections of the ACTE flaps after landing were not significantly different than they were before flight. Aside from a flight with a 10-deg ACTE flap setting, changes were within understood accuracy of the scanning system.

III. ACTE Aerodynamic Modeling Efforts

A model of the aerodynamic effects of the ACTE flaps was created before the flight tests and incorporated into a six-degree-of-freedom GIII simulation to support flight readiness reviews and pilot training. The ACTE aerodynamic model was made in the form of force and moment coefficient increments that are added to the baseline GIII aerodynamic model. The baseline GIII aerodynamic model was built mostly from flight data from a series of flights with the testbed airplane prior to installation of the ACTE flaps. Some pieces of the baseline model, such as the elevator tab effectiveness, could not be derived from the baseline flight data. These pieces were filled in using a preexisting GIII aerodynamic model. Modeling efforts assumed that the zero-degree ACTE flap configuration was the

same as the baseline GIII airplane with zero Fowler flap deflection. All modeling efforts used wing and ACTE flap shapes that did not account for deflections from in-flight aerodynamic loads.

In order to meet project milestones, the complexity of the ACTE aerodynamic model evolved over time. The run matrices for full potential and Navier-Stokes CFD were broken up into sets based on priority, so that work could be performed on some of the results without having to wait for all of the runs to be completed. This staging of runs helped to meet the schedule of design and flight readiness reviews, in addition to the creation of intermediate aerodynamic models. The first version of the ACTE aerodynamic model was based on vortex lattice and empirical data and was created while the CFD work was underway. One set of Navier-Stokes CFD results at Mach 0.85 was used to provide guidance on the compressibility effects. The second version of the model was built from a mixture of full potential and Navier-Stokes CFD results. The final version of the ACTE model was built solely from the Navier-Stokes results. Roughly two years passed between the creation of the initial and final versions of the aerodynamic model. The four tools used to predict the aerodynamic effects of the ACTE flaps are described in the following subsections.

A. Digital Datcom

The first tool used to model the effects of the ACTE flaps was the United States Air Force (USAF) Stability and Control Digital Datcom,[3] which is a software implementation of the very large Datcom report.[4] For the purposes of this report, the terms "Datcom" and "Digital Datcom" are used somewhat interchangeably. The Datcom consists of methods for calculating aerodynamic characteristics for airplanes based on aerodynamic theory, wind tunnel data, and flight data. The software version automates the extensive calculations and table lookups that Datcom requires. Airplane configuration is specified using geometric parameters; no grids or flow solutions are involved. The ACTE flaps were modeled in Datcom as plain flaps. The transition sections could not be modeled and were included as part of the flap area. In general, Datcom does not have limitations in ranges of speed, angles of attack, or flap deflections; but its methods are not applicable to every combination of geometry and flight condition. Computed flap effects in Digital Datcom are not dependent on wing incidence angle, twist, or dihedral. Flap calculations also do not consider parts of the airplane other than the wing.

In this report, Digital Datcom was used to predict flap effects for a matrix of Mach numbers 0.2 to 0.85 at altitudes of 10-, 20-, 30-, and 40-thousand feet above sea level. Analysis of each flight condition was performed with a separate Digital Datcom run. The program has the ability to do multiple flight conditions in a single execution, using one of two user-selected styles, but it was found to produce markedly different pitching moment increment results depending on which style is picked. Digital Datcom only produces pitching moment increments at speeds up to where it starts employing transonic methods, which in this case was Mach 0.6.

B. Athena Vortex Lattice

The second analysis tool was a vortex lattice program, Athena Vortex Lattice (AVL).[5] The AVL program is useful for quickly generating aerodynamic data, though its applicability is limited to small angles of attack because of its basic small perturbation and linearized inviscid incompressible flow assumptions. Compressibility effects are added using the Prandtl-Glauert correction. An illustration of an AVL model for the test airplane with ACTE flaps deflected 25 deg is shown in Fig. 5. The flaps were modeled by breaking the wing surface at the flap/aileron hinge line. The aft portion of the wing was then broken at the edges of the center portion of the flap and the edges of the transition sections. The aileron was also broken out as a separate surface. Breaking up the wing surface this way makes it possible to get better vortex panel distributions at the edges of all the surfaces.

Surfaces edges are modeled in AVL with a constant height. Surface inclinations with respect to freestream airflow are set using the combination of an overall surface incidence angle and incidence angles specified for each edge. The ACTE flap deflections were set by specifying the incidence angles of the center flap edges and the corresponding edges of the transition sections. The transition section edges that connect to the wings were left at zero incidence, which mimics the physical behavior of the transition sections. The resulting trailing edge incidence distribution can be seen in Fig. 5. The rest of the wing was treated as a flat plate at the wing incidence angle, without accounting for twist and without any airfoil sections specified to AVL.

It should be noted that the vortex lattice model used for the work presented in this paper is more complex than what was originally used for the ACTE modeling efforts, in order to provide a better assessment of the AVL capabilities. For this report, AVL results were generated at points corresponding to the Mach numbers, altitudes, and

angles of attack of the flight-test points, to provide direct comparisons to flight results. Additional runs were performed to fill out Mach number ranges for each flap setting, so that comparisons could be made to the other tools at conditions that were not experienced in flight.

C. TRANAIR

The next aerodynamic analysis tool that was used, in terms of analysis complexity, was TRANAIR (Calmar Research Corporation, Cato, New York), which is a full potential flow solver.[6] TRANAIR produces solutions much faster than a Navier-Stokes solver, while able to treat more complex flows and airplane geometries than the vortex lattice approach. Viscous effects are included from implicit coupling with a boundary layer code. TRANAIR requires the specification of a surface grid for the airplane, but not a volume grid. The program then generates a Cartesian unstructured volume grid internally, with error-based mesh refinement while it is executing. Wake regions need to be explicitly defined. An example of a TRANAIR surface grid, with wake regions, is shown in Fig. 6. For clarity, the stabilizer wake regions are not shown in Fig. 6. While the full potential flow analysis approximation is applicable across the full range of airplane speeds and geometries, TRANAIR is generally used for cases where flow is attached.[7] The limitation of flow attachment reduces the range of ACTE flap deflections for which the code is appropriate. Reference 7, published after the ACTE work was completed, proposes a means to extend TRANAIR to separated flows.

D. STAR-CCM+

The most complex aerodynamic analysis tool used for this study was STAR-CCM+ (CD-Adapco, Melville, New York), an unstructured full Navier-Stokes finite volume CFD code. Full Navier-Stokes solutions are generally not considered to be limited to any speed, angle of attack, or flap deflection range, but each solution takes significantly more computing time than the simpler analysis methods used in this work. The STAR-CCM+ program was previously used to analyze a proposed wing-glove experiment for the GIII testbed airplane.[8] An example of a STAR-CCM+ surface mesh for the GIII airplane with ACTE flaps is shown in Fig. 7. The full airplane was modeled so that sideslip effects could be determined. Run times could have been shortened for cases with no sideslip by only modeling half the GIII airplane and using a symmetry plane. Engines were modeled using flow conditions obtained from an engine cycle model.

Grids used for the STAR-CCM+ work were comprised of roughly thirty-five million finite volume cells. It was found that this mesh size was generally sufficient to provide grid-independent solutions for the airplane aerodynamic coefficients. Far field grids used unstructured polyhedral meshes. Near-wall grids utilized prism layers to better model the boundary layer. Turbulence was modeled using the Shear Stress Transport k-omega two-equation model with an all-y+ wall treatment. Second-order Roe flux difference splitting was used with a coupled implicit flow solver.

IV. Flight Results and Discussion

The ACTE flight-test series spanned 23 flights, with ACTE flap deflections of -2, 0, 2, 5, 10, 12.5, 15, 17.5, 20, 25, and 30 deg. Flap settings of 5 deg and below were flown up to Mach 0.75 at an altitude 40,000 ft MSL. As flap deflection increased beyond 5 deg, the flight envelope was progressively reduced. The results for the 12.5- and 17.5-deg deflections are omitted from this report, as the flaps could not be set precisely at those angles, and there were no CFD runs performed for those deflections. Additional information about the ACTE flights can be found in Ref. 1.

A. Data Analysis Approach

The main aerodynamic characteristics of interest for this work were the nondimensional lift and pitching moment coefficients. Since thrust measurements were not available, drag could not be accurately determined. The effects of thrust were negligible for the other terms. The analysis tools predicted that deflection of the ACTE flaps would cause changes to the GIII lateral-directional aerodynamics. These changes were predicted to be small, however, and were not discernable in the flight data, due to scatter.

Lift coefficient, C_L, and pitching moment coefficient, C_m, increments due to ACTE flaps were determined using stability and control parameter estimation results. Computing the increments using parameter estimation results instead of steady-state test points makes it possible to compensate for differences in trim elevator and angle of attack between maneuvers. The following linear model shown in Eq. (1) was used for the coefficients:

$$C_L = C_{L_B} + C_{L_\alpha}\alpha + C_{L_q}\frac{q\bar{c}}{2V_\infty} + C_{L_{de}}de \tag{1}$$

Pitching moment coefficient used the same model setup. The term C_{L_B} is a bias term that is different than the airplane C_{L_0} because it comes from the linearization of the aerodynamics and contains the aerodynamic contributions of the deflected stabilizer, elevator tab, and ACTE flaps. The bias term can also collect the effects of measurement biases. The coefficients in the lift and pitching moment models were estimated using standard equation error[9] and output error[10] techniques. The maneuvers used for parameter estimation were piloted 2-1-1 inputs, performed in sets of three.

The estimated pitching moment bias term, $\hat{C}_{m_B}$, had to be adjusted for elevator tab effects because the tab position was not the same for every maneuver. The elevator tab contribution to C_L is small, but for C_m, it is significant. Although the elevator tab position was measured, it remained fairly constant during the 2-1-1 maneuvers and, as such, tab effectiveness derivatives could not be identified. Tab settings were also highly correlated to flight condition and trim elevator position, so estimation of tab effectiveness from a global data set was not possible. Since the elevator tab effectiveness could not be estimated from flight data, the tab contributions were removed from the bias term estimates using values from the baseline GIII aerodynamic model. The stabilizer contributions to lift and pitching moment were not removed, since all configurations used the same stabilizer position.

The lift coefficient increment due to ACTE flaps, ΔC_L, was calculated from the parameter estimation results using Eq. (2):

$$\Delta C_L = \hat{C}_{L_{B,2}} - \hat{C}_{L_{B,1}} + \alpha_2\left(\hat{C}_{L_{\alpha,2}} - \hat{C}_{L_{\alpha,1}}\right) \tag{2}$$

The subscript "2" denotes the estimates for when the ACTE flaps were deflected, and "1" denotes the estimates for when the flaps were not deflected. The term α_2 is the average angle of attack for the flaps-deflected maneuver. The definition of ΔC_L is illustrated in Fig. 8. Note that the average angles of attack in the figure are closer to the nonlinear C_L range than would be typical during parameter estimation maneuvers to exaggerate the differences between the measured C_L curves and the linear models. The ΔC_L amounts to the difference between the estimated lift of the GIII airplane with deflected ACTE flaps at α_2 and the predicted lift of the GIII airplane with non-deflected ACTE flaps at that same angle of attack. For high flap deflections, α_2 could be lower than the minimum angle of attack experienced during the flaps-not-deflected maneuvers. The pitching moment increment, ΔC_m, was computed the same way as ΔC_L.

Parameter estimation maneuvers were typically flown in sets of three. To reduce the number of points for presentation, results from the three maneuvers at each test point were blended into a weighted mean based on their individual standard errors. Confidence bounds were computed using estimated standard errors for the weighted means and ordinary uncertainty analysis calculations[11] shown in Eq. (3):

$$U^2_{\Delta C_L} = \hat{\sigma}^2_{\hat{C}_{L_{B,2}}} + \hat{\sigma}^2_{\hat{C}_{L_{B,1}}} + \left(\alpha_2\hat{\sigma}_{\hat{C}_{L_{\alpha,2}}}\right)^2 + \left(\alpha_2\hat{\sigma}_{\hat{C}_{L_{\alpha,1}}}\right)^2 \tag{3}$$

The uncertainty calculation in Eq. (3) does not include uncertainties in the angle of attack or other measurements. The equation also does not include the covariance between $\hat{C}_{L_B}$ and $\hat{C}_{L_\alpha}$, which would tend to be a negative number, reducing the overall uncertainty.

B. Comparisons of Flight Results to Predictions

The use of parameter estimation results to compute the ACTE flap lift and pitching moment increments worked well. Output error and equation error can produce different results, due to different sensitivities to measurement errors. For example, scale errors in angle of attack are sometimes ignored by output error, but lead directly to scale errors in equation error estimates of angle-of-attack derivatives. Differences between the two estimation techniques were used

to guide data processing requirements, until the two techniques agreed as well as possible. For this work, the remaining differences were largest at each end of the Mach number range, particularly the low end, and are thought to be due to the angle-of-attack calibration and/or unresolved time shifts in the measured data. For ACTE flap deflections of 10 deg and greater, the differences in ΔC_L between the two techniques were 6 percent or less, and the differences in ΔC_m were less than 10 percent. The results presented in this report are from output error, as they had less scatter than the equation error results, and the estimated Cramér-Rao bounds were more consistent than the estimated standard errors of the equation error results. The equation error estimates of ΔC_L and ΔC_m were within the scatter of the results that will be presented, with the exception of the high-speed ΔC_m estimates for an ACTE flap deflection of -2 deg.

Figure 9 shows estimated lift coefficient models from flight data for all ACTE flap deflections at Mach 0.3 and an altitude of 10,000 ft MSL. Figure 9 is analogous to the ΔC_L illustration of Fig. 8. The angle-of-attack ranges that are shown correspond to those of the maneuvers used. For flap deflections greater than 15 deg, the average angles of attack for the flaps-deflected maneuvers were lower than the angle-of-attack range of the non-deflected data, so the C_L values for non-deflected flaps are entirely extrapolation.

Figure 10 shows the ΔC_L predictions from the four analytical tools, in comparison to a confidence region representing estimates from flight data using parameter estimation results and Eq. (2). The confidence region corresponds a 95 percent (2-σ) confidence region and includes variation in the ΔC_L estimates due to Mach number and altitude, as well as the scatter in the individual parameter estimation results. The variation in TRANAIR and STAR-CCM+ results at each ACTE flap deflection is due to changes in angle of attack, Mach number, and altitude. For simplicity, the AVL and Digital Datcom results are only shown as trends in Fig. 10. All four analysis tools provide estimates that match flight data well for small ACTE flap deflections. The predictions start to fall out of the flight data confidence region as flap deflection increases, with the flight results showing a smaller increase in lift due to the flaps than the analysis tools predicted. The static pressure measurements discussed in Ref. 1 indicate that the STAR-CCM+ solutions underpredicted the flow separation over the flaps. The AVL results, not expected to be good for large deflections, actually match the TRANAIR and STAR-CCM+ results well up to a deflection of 15 deg. The TRANAIR and STAR-CCM+ results agree well with each other up to 20 deg. Digital Datcom predicted the diminishing effectiveness of the flaps fairly well and did a good job of predicting ΔC_L overall. Recall that the Datcom model included the transition sections as parts of the flap geometry. If the transition sections are not included in the Datcom model, the predicted ΔC_L values are lower than the flight results. Averaging the two sets of results produces ΔC_L predictions that match the flight results very well, suggesting an approach for dealing with the transition sections in Datcom.

Figure 11 shows comparisons of predicted ΔC_m values to a confidence region based on flight parameter estimation results. Not reflected in the confidence region is the uncertainty in the elevator tab contributions to C_m. The TRANAIR and STAR-CCM+ results, again, agree very well with each other. The spread in the STAR-CCM+ results for flap deflections of 15 and 30 deg is due to the wide range of Mach numbers and angles of attack that were analyzed. Though the AVL results are in the confidence region up through 15 deg of deflection, they follow a different trend than the others, showing an increasing negative slope with increasing flap deflection. With exception to flap settings of 5 deg and below, the Digital Datcom results do not match the flight results very well, exhibiting a much steeper slope than the two CFD programs. The different slope in ΔC_m might be due to the Digital Datcom internal calculations placing the lift increment at the wrong location. A moment arm of one to two feet is enough to account for the differences in ΔC_m slope shown between Datcom and the other tools. Note that Digital Datcom does not use its prediction of ΔC_L to compute ΔC_m. Leaving the transition sections out of the Datcom model does not change ΔC_m enough to match the other data.

Estimates of ΔC_L for ACTE flap deflections of up to 10 deg are shown again in Fig. 12, this time as a function of Mach number. The flight results are shown as shaded areas that correspond to 2-σ confidence regions for each flap deflection. For some Mach numbers, there were test points at multiple altitudes. The TRANAIR and STAR-CCM+ results agree very well with each other across the Mach range, with some sporadic outliers and some noticeable mismatches at Mach 0.85 for a flap deflection of 5 deg. The AVL results match the two CFD codes up through Mach 0.8. Datcom predicts a slight reduction in flap effectiveness with Mach number, until around Mach 0.6, when it starts to include transonic effects.

The estimates of ΔC_m are shown versus Mach number in Fig. 13. For ACTE flap deflections of 2 and 5 deg, the predicted results match the flight results well. For a deflection of -2 deg, the predictions follow the trend of the flight

results, but are on the edge of the confidence region. The STAR-CCM+ and TRANAIR results agreed well with each other, except for a significant mismatch at Mach 0.3 for a deflection of 10 deg. The AVL predictions had similar trends with Mach number as the CFD methods, but the CFD methods predicted stronger compressibility effects. The jaggedness in the AVL curves is due to having solutions for multiple angles of attack at each Mach number, corresponding to the trim angles of attack at the altitudes of the flight data. As mentioned previously, pitching moment predictions from Digital Datcom were only given for a subset of Mach numbers. No significant Mach trend was shown in the Datcom predictions of ΔC_m.

Overall, the results indicate that the simpler tools would have provided adequate data for modeling the ΔC_L and ΔC_m due to ACTE flaps at small deflections and low Mach numbers, potentially eliminating the need for CFD runs at those conditions. While the ΔC_L predictions from Digital Datcom were good across the full range of flap deflections, they did not match the Mach number trends of the flight results as well as the other tools. The significant mismatches between flight data and the Datcom predictions of ΔC_m cause some concern for using Digital Datcom as a standalone modeling tool for this application. The AVL results for both ΔC_L and ΔC_m were comparable to the CFD results up to Mach 0.8 for small flap deflections. The TRANAIR ΔC_L and ΔC_m results were very similar to the STAR-CCM+ results for nearly the full Mach range and for ACTE flap deflections of up to around 20 deg, which suggests that TRANAIR could suitably model the ACTE flaps for most conditions. In all, the results of these modeling efforts suggest that, for this project, Navier-Stokes flow solutions could have been targeted toward large flap deflections and toward high Mach numbers. This finding supports the approach that was used to generate the aerodynamic model for the ACTE flaps.

V. Conclusion

Adaptive compliant trailing edge (ACTE) flaps were installed on a GIII testbed airplane, and a series of research flights was flown. Prior to the flights, several analysis tools were used to predict the aerodynamic effects caused by the flaps. The analysis tools varied in level of complexity. Lower complexity tools were used while full potential and full Navier-Stokes flow analyses were being performed. The lower complexity tools were Digital Datcom and a vortex lattice program, Athena Vortex Lattice (AVL). The full potential solutions were generated with TRANAIR, while the Navier-Stokes solutions were performed with STAR-CCM+.

Lift and pitching moment coefficient increments due to the ACTE flaps were estimated from flight data using parameter estimation results. The estimated aerodynamic increments were compared to the results from the predictive tools. It was found that all the tools used for this study predicted lift coefficient increments that matched flight data well for small flap deflections. At large flap deflections, all of the tools overpredicted the lift coefficient increments. The vortex lattice code matched the full potential and Navier-Stokes results very well for flap deflections up to roughly 15 deg for Mach numbers up to Mach 0.8. Only Digital Datcom and STAR-CCM+ predicted the reduction in flap effectiveness that occurred as deflection magnitude increased. While Datcom produced good predictions of lift coefficient increments for all flap deflections, it did not do as good of a job matching Mach trends. Errors in the pitching moment increment results also cause some concern with using Digital Datcom as a standalone modeling method. The estimates of pitching moment increments from TRANAIR and STAR-CCM+ had the best agreement with the flight results. The predicted lift and pitching moment increments from TRANAIR and STAR-CCM+ agreed well with each other up to Mach 0.85, but only for flap deflections of less than 20 deg.

The results of this work suggest that the lower-complexity analysis tools could provide adequate modeling of the compliant trailing edge flaps for small-magnitude flap deflections. It may be possible to reserve computationally intensive full Navier-Stokes solutions for cases involving large flap deflections or high Mach numbers. The results support the methodology that was used to create the aerodynamic model for the ACTE flaps and could be used to guide modeling efforts for similar projects.

References

[1]Cumming, S. B., Smith, M. S., Ali A. N., Bui, T. T., Ellsworth, J. C., and Garcia, C. A., "Aerodynamic Flight Test Results for the Adaptive Compliant Trailing Edge," AIAA 2016-#### (to be published), 2016.

[2]Baumann, E., Hernandez, J., and Ruhf, J. C., "An Overview of NASA's SubsoniC Research Aircraft Testbed (SCRAT)," NASA TM-2013-216595, 2013.

[3]Williams, J. E., and Vukelich, S. R., "The USAF Stability and Control Digital Datcom," AFFDL-TR-79-3032, 1979.

[4]Finck, R. D., "USAF Stability and Control Datcom," AFWAL-TR-83-3048, 1978.

[5]Athena Vortex Lattice (AVL), Software Package, Ver. 3.35, URL: http://web.mit.edu/drela/Public/web/avl/ [cited 29 April 2016].

[6]Samant, S. S., Bussoletti, J. E., Johnson, F. T., Burkhart, R. H., Everson, B. L., Melvin, R. G., Young, D. P., Erickson, L. L., Madson, M. D., and Woo, A. C., "TRANAIR: A Computer Code for Transonic Analyses of Arbitrary Configurations," AIAA 87-0034, 1987.

[7]Young, D. P., Melvin, R. G., Huffman, W. P., Arian, E., Hong, M., and Drela, M., "Implementation of a Separated Flow Capability in TRANAIR," *AIAA Journal*, Vol. 52, No. 8, 2014, pp. 1699-1716.

[8]Bui, T. T., "Analysis of Stall Aerodynamics of a Swept Wing with Laminar-Flow Glove," *Journal of Aircraft*, Vol. 52, No. 3, 2015, pp. 867-871.

[9]Morelli, E. A., "Practical Aspects of the Equation-Error Method for Aircraft Parameter Estimation," AIAA 2006-6144, 2006.

[10]Maine, R. E., and Iliff, K. W., "Application of Parameter Estimation to Aircraft Stability and Control–The Output-Error Approach," NASA RP-1168, 1986.

[11]Coleman, H. W., and Steele, W. G., "Experimentation and Uncertainty Analysis for Engineers," John Wiley & Sons, Inc., New York, 1999.

Figures

Figure 1. Test airplane in flight with ACTE flap deflection of 25 deg.

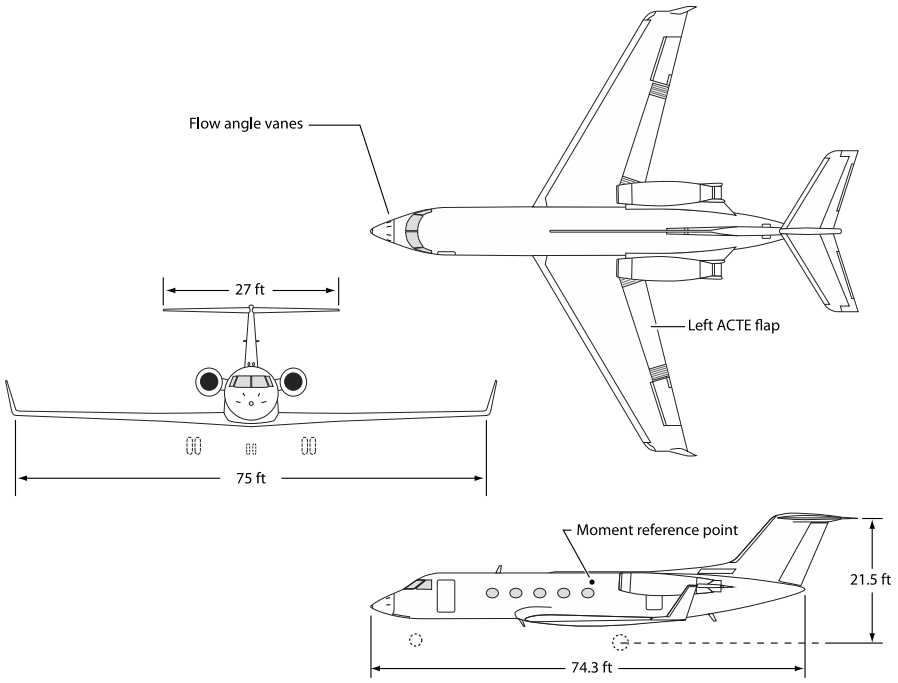

Figure 2. Three-view drawing of the GIII airplane.

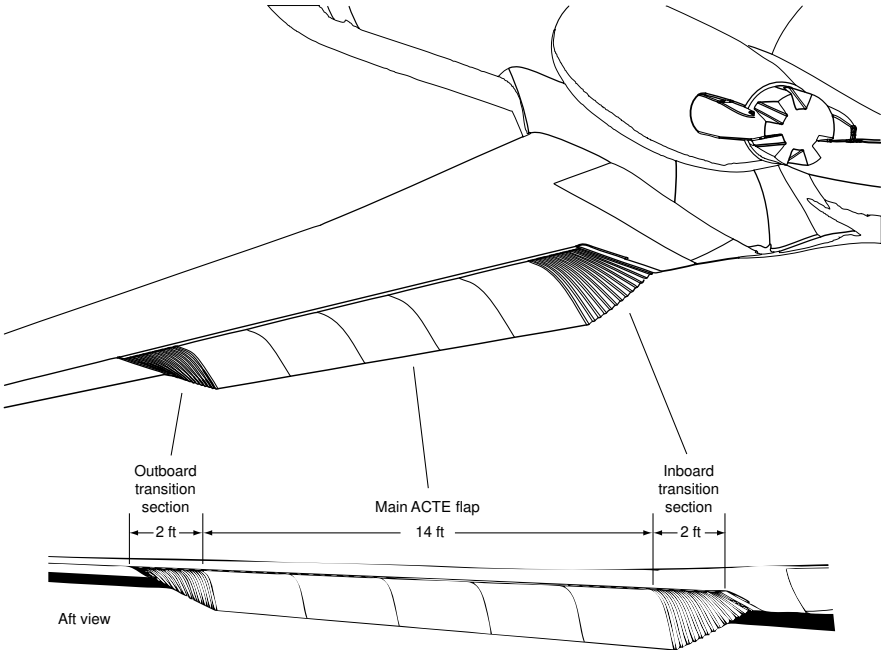

Figure 3. Illustration of the left ACTE flap (deflection of 30 deg).

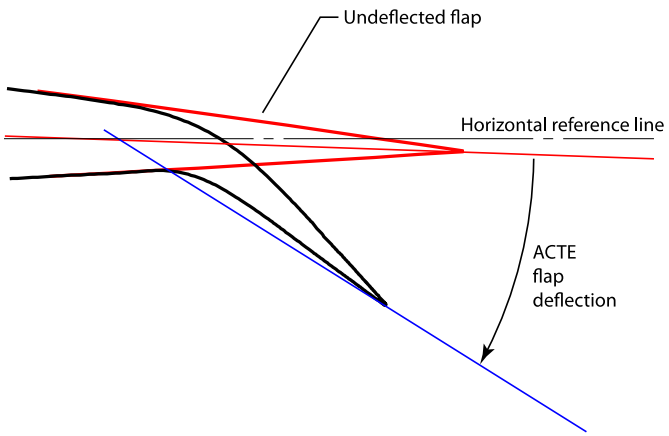

Figure 4. Definition of ACTE flap deflection.

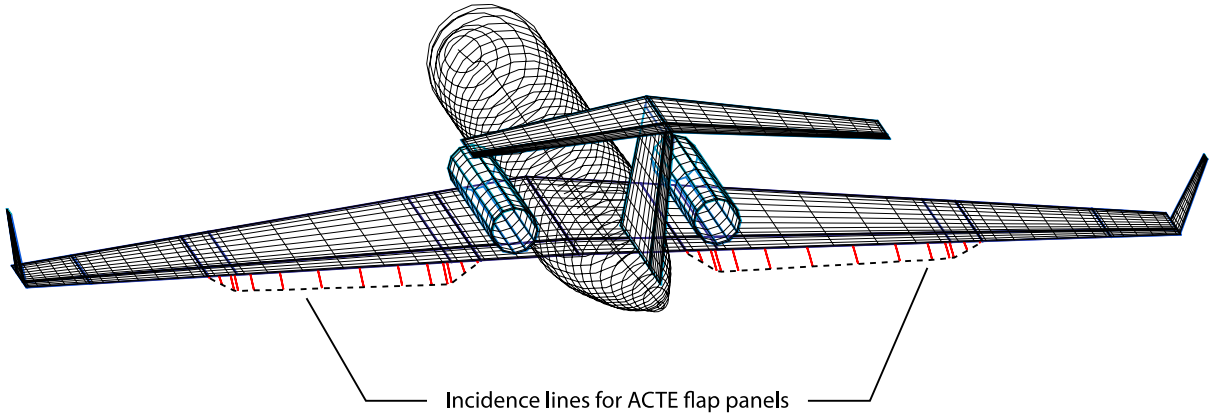

Figure 5. AVL panel layout (ACTE flap deflection of 25 deg).

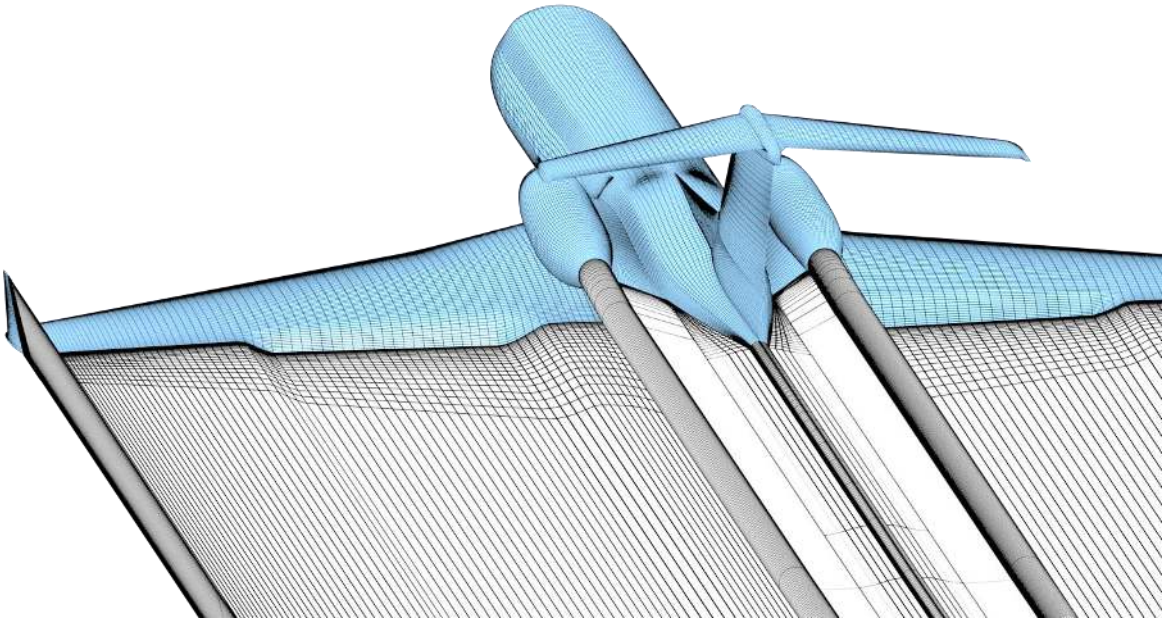

Figure 6. TRANAIR surface and wake grids.

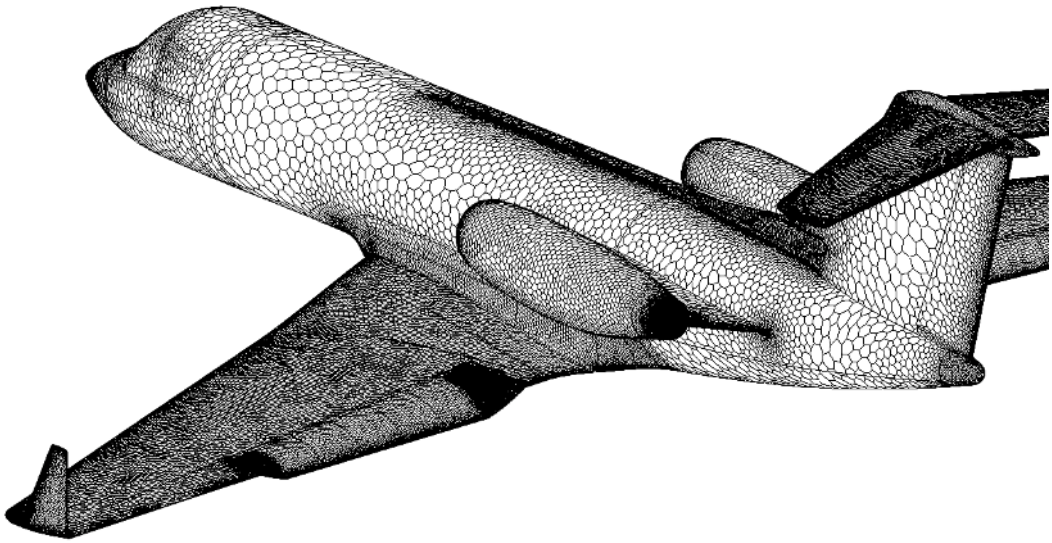

Figure 7. STAR-CCM+ surface mesh.

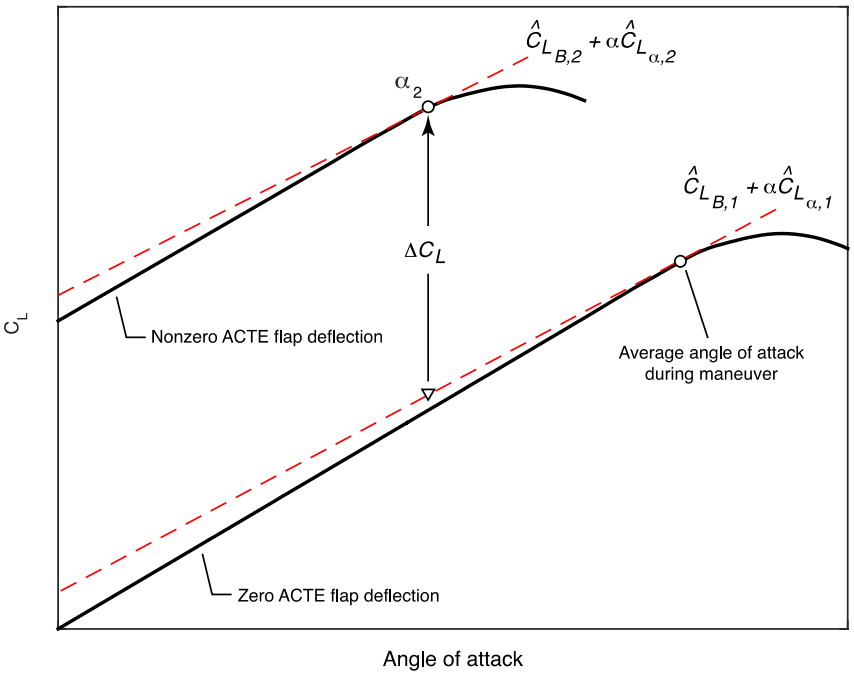

Figure 8. Definition of lift coefficient increment.

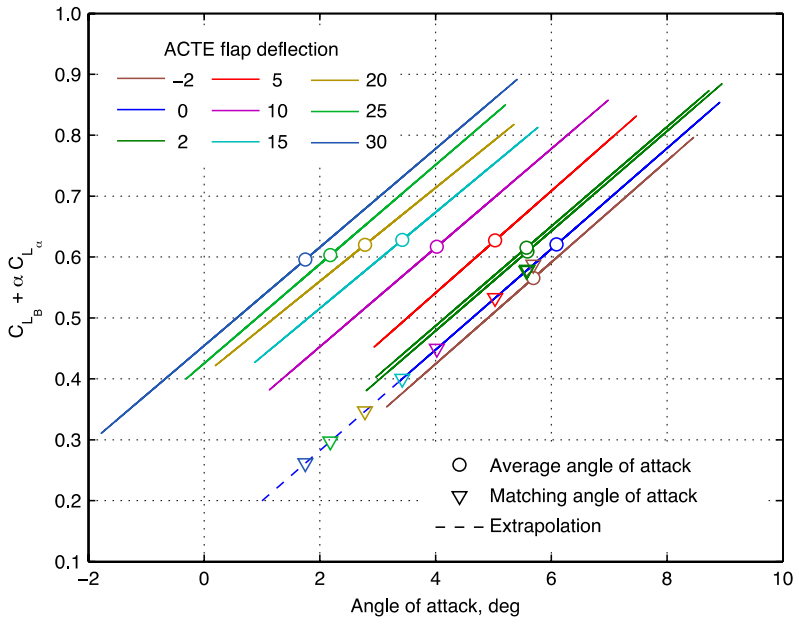

Figure 9. Estimated lift coefficient models from flight data for Mach 0.3 at 10,000 ft altitude.

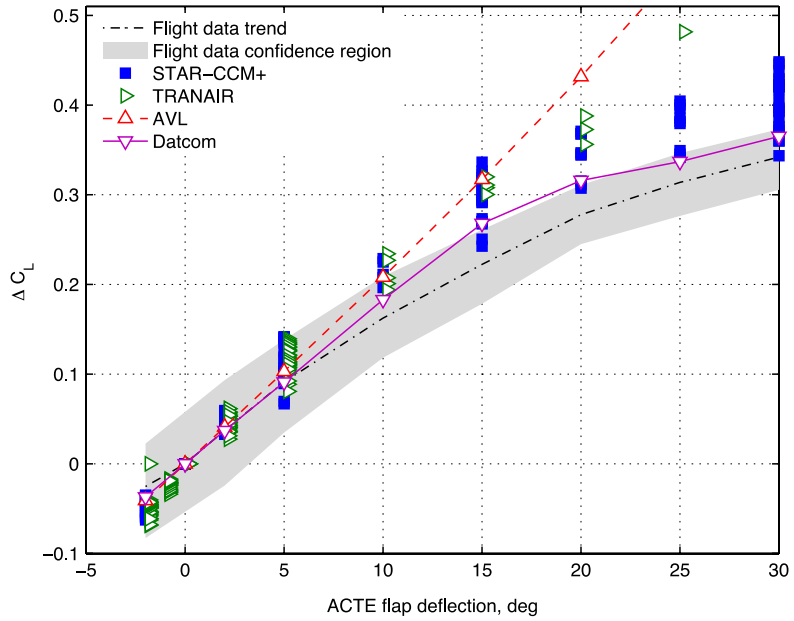

Figure 10. Estimated lift coefficient increments versus ACTE flap deflection.

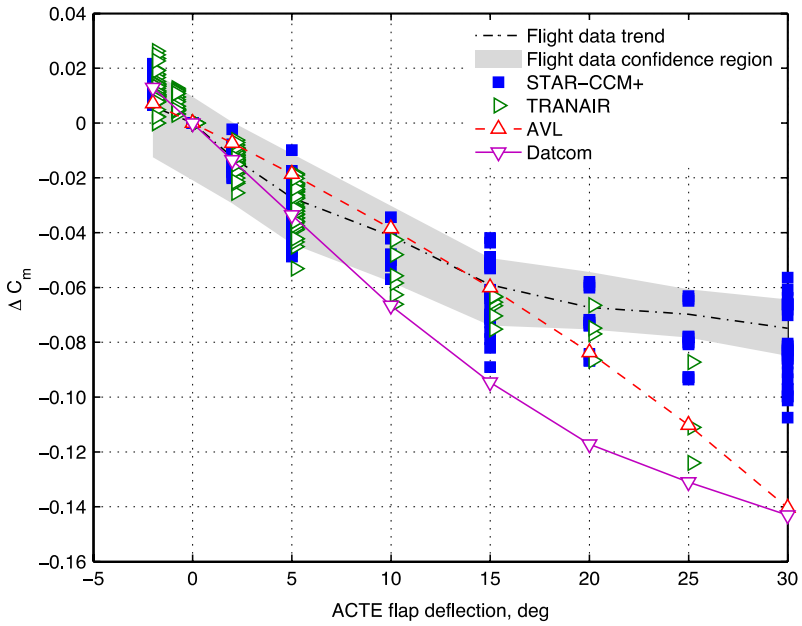

Figure 11. Estimated pitching moment coefficient increments versus ACTE flap deflection.

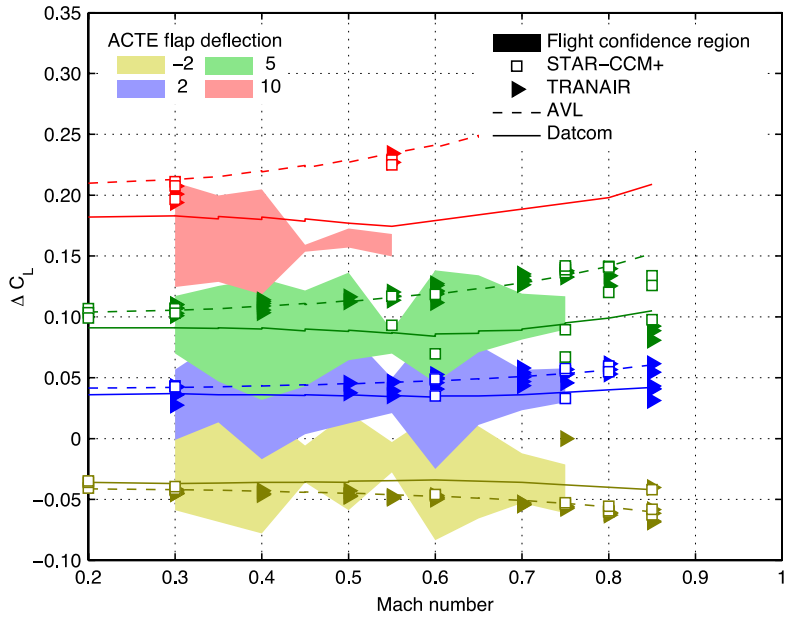

Figure 12. Estimated lift coefficient increments versus Mach number.

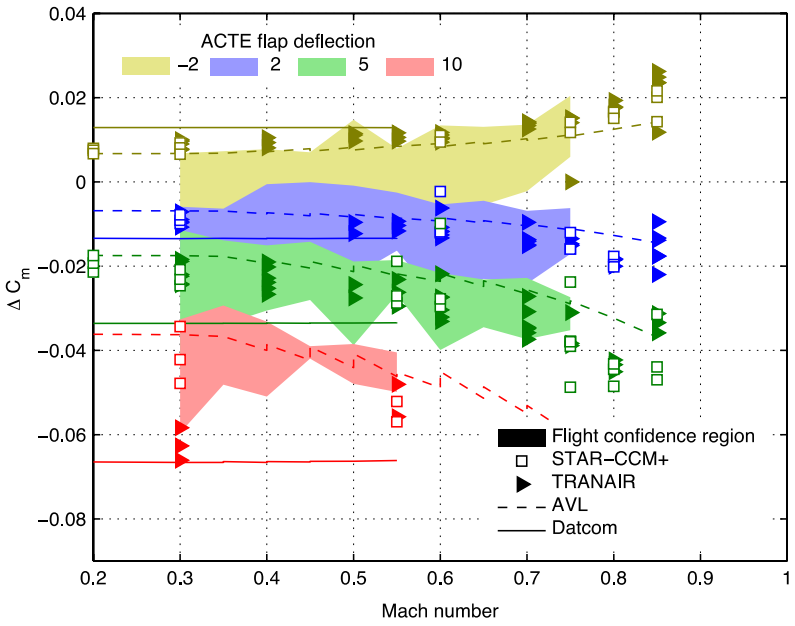

Figure 13. Estimated pitching moment coefficient increments versus Mach number.